Tarchichi N., Chollet F., Manceau J.-F., "New regime of droplet generation in a T-shape microfluidic junction"
Journal of Microfluidics and Nanofluidics, doi:10.1007/s10404-012-1021-8, Vol. 14, No. 1 (2013) : 45-51

New regime of droplet generation in a T–shape microfluidic junction

Nathalie TARCHICHI · Franck CHOLLET · Jean-François MANCEAU

2012

Abstract We present an experimental study of a new regime of monodisperse micro–droplet generation that we named the balloon regime. A dispersion of oil in water in a T–junction microfluidic system was studied. Several microfluidic devices having different cross–sections of the continuous and the dispersed phases micro–channels were tested. This new regime appears only for low dispersed phase velocity. The micro–droplet size is mainly related to the geometry of the T–junction micro–channels especially its width and depth, and independent of the continuous and dispersed phases velocities. In our experiments, the velocities of the continuous and the dispersed phases $\overline{v}_c$ and $\overline{v}_d$ respectively, have been varied in a wide range: $\overline{v}_c$ from 0.5 to 500 mm/s, and $\overline{v}_d$ from 0.01 to 30 mm/s. We show that the continuous phase only controls the micro–droplet density, while the dispersed phase linearly changes the frequency of the micro–droplet generation. Another particularity of the present regime, which differentiates it from all other known regimes, is that the micro–droplet retains its circular shape throughout its formation at the T–junction, and undergoes no deformation due to the drag forces. We propose a mechanism to explain the formation of micro–droplets in this new regime.

Keywords microfluidics · T–Junction · monodisperse droplet · generation regime · liquid–liquid system

Nathalie TARCHICHI · Franck CHOLLET · Jean-François MANCEAU
FEMTO-ST Institute, Université de Franche-Comté, 32 avenue de l'Observatoire, 25044 Besançon, FRANCE
E-mail: franck.chollet@femto-st.fr

1 Introduction

Monodisperse liquid–droplets or gas–bubbles have recently been used in various fields such as photonics (Hashimoto et al 2006), sensors (Nguyen et al 2007), biomedical (Seong et al 2002), chemical process (Gunther et al 2005), etc. For these applications it is generally necessary to control precisely the geometry of the generated droplets or bubbles. Their generation is then based on microfluidic devices using different principles: T–junction (Thorsen et al 2001), flow–focusing (Gañán-Calvo and Gordillo 2001), or co–flowing devices (Umbanhowar et al 2000). In each case, the mechanism of formation of droplet or bubble is strongly related to the microfluidic structure (Abate et al 2009). In the flow–focusing and the co–flowing devices, the droplet or bubble generation depends on the inertia of the fluids (Cubaud et al 2005; Fu et al 2009). In the T–junction devices, the droplet or bubble generation is controlled by the shear force and the interfacial force (Nisisako et al 2002). The shear force acts on the interface between the two fluids driving the generation of droplets or bubbles. The capillary number Ca, reflecting the ration between the shear force and the interfacial force is a parameter commonly used to characterize these phenomena. Based on the value of the capillary number, three main regimes of generation of droplets or bubbles are present: squeezing, dripping and jetting regimes (Cubaud and Mason 2008; Christopher et al 2008; Sivasamy et al 2011; Menech et al 2008; Glawdel et al 2012). The squeezing regime is observed for low values of Ca. The droplet or bubble generation occurs at the two phases intersection. In this regime, the droplets or bubbles generated have an elongated shape in the continuous phase micro-channel. The size of these plugs depends mainly on the flow rate of the

dispersed phase Q_d and the continuous phase Q_c, and is independent of Ca, as the dominant force is the interfacial force. The length L of these plugs is given by: $\frac{L}{w_c} = 1 + \alpha\frac{Q_d}{Q_c}$, with w_c the width of the continuous phase channel and α a constant depending on the geometry of the T–junction microfluidic system (Garstecki et al 2006). The dripping regime is observed for higher values of Ca. In this regime, the droplets or bubbles generated do not occupy the entire width of the continuous phase micro-channel and are smaller than the width of the continuous phase channel. The size of these droplets or bubbles is a function of Ca, as the viscous drag force is the dominant force controlling the detachment of the droplet or bubble which occurs just after the intersection of the two phases (figure 1). The diameter d of these droplets is given by: $\frac{d}{d_i} \propto \frac{1}{Ca}$, with d_i the cross–section dimension of the channel (Cristini and Tan 2004). The jetting regime is a regime of droplet or bubble generation in which the dispersed phase forms a long neck in the channel of the continuous phase. The droplet or bubble formation occurs downstream at some distance from the T–junction. This regime has the advantage of generating droplets or bubbles of small size, but when the droplets or bubbles become very small compared to the width of the continuous phase channel, the jetting regime become unstable. The exact value of the capillary number Ca giving the various regimes, and the equations linking the size of the droplets or bubbles to that number in the dripping and the jetting regimes, depend on the experimental conditions such as the geometry of the T-junction device (width of the continuous phase channel, depth of the channels, etc), and the physical properties of the fluids (viscosity, surface or interfacial tension, etc).

In this work, we show the presence of a new regime of generation of droplets in which the droplet size depends mainly on the micro-channels geometry and is independent of Ca. The droplet diameter does not change when the velocity of the continuous phase $\overline{v}_c$ or the velocity of the dispersed phase $\overline{v}_d$ change. The continuous phase is just the carrier of the droplet. The dispersed phase control the droplet frequency.

2 Microfluidic system

The micro-droplets were generated using a T-junction microfluidic device made on silicon-glass. The preparation of these samples goes through five main stages: over–side photolithography using SPR220 photoresist, micro-channels etching by Deep Reactive Ion Etching (DRIE), back side photolithography using AZ9260 photoresist, through hole etching, and anodic bonding with glass. The wafer was subsequently diced into 12 chips.

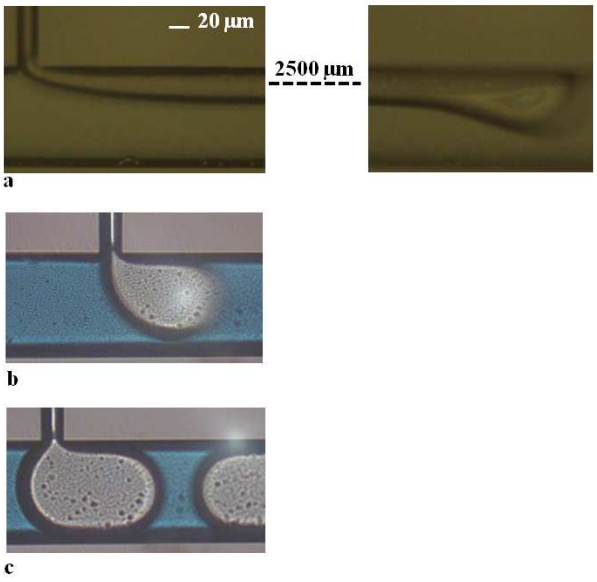

Fig. 1 View of the jetting regime (a), the dripping regime (b) and the squeezing regime (c), with $w_c = 100$ µm, $w_d = 20$ µm, $\overline{v}_d = 20$ mm/s and $\overline{v}_c = 50$ mm/s (a), $\overline{v}_d = 12$ mm/s and $\overline{v}_c = 14$ mm/s (b), $\overline{v}_d = 12$ mm/s and $\overline{v}_c = 2.3$ mm/s (c).

The width of the perpendicular channel w_d and the width of the main channel w_c were varied from one chip to another ($w_d = 10$, 20 and 50 µm, $w_c = 50$ and 100 µm). The micro-channel depth was controlled after etching by an Alpha-step surface profiler and was 23, 46 and 72 µm. All microfluidic devices used in this work were fabricated in the clean room MIMENTO of the Femto-st institute.

We used silicone oil (Dow Corning 704® with kinetic viscosity of 39 cst, and a density of 1070 kg/m^3), as the dispersed phase, and deionized water colored with a blue food dye as the continuous phase. The interfacial tension oil-water was 100 mN/m without surfactant and was measured with a KRÜSS tensiometer. This high value of the interfacial tension is probably due to the use of ultra pure oil. Actually, the higher the purity of the fluid, the higher the interfacial tension (Dopierala et al 2011). Two syringe pumps were used to inject liquids and control the flow rates of the continuous and dispersed phases in the micro-channels. For very low flow rate a leek was introduced at the chip input. Micro–droplets diameter was measured using a microscope and a CCD camera with a high speed shutter (figure 2). All experiments were realized at a constant temperature (20 ± 2°C). Performing the experiment at a constant temperature is essential, because it critically influences the physical properties of the fluids, specially their viscosities, and the interfacial tension.

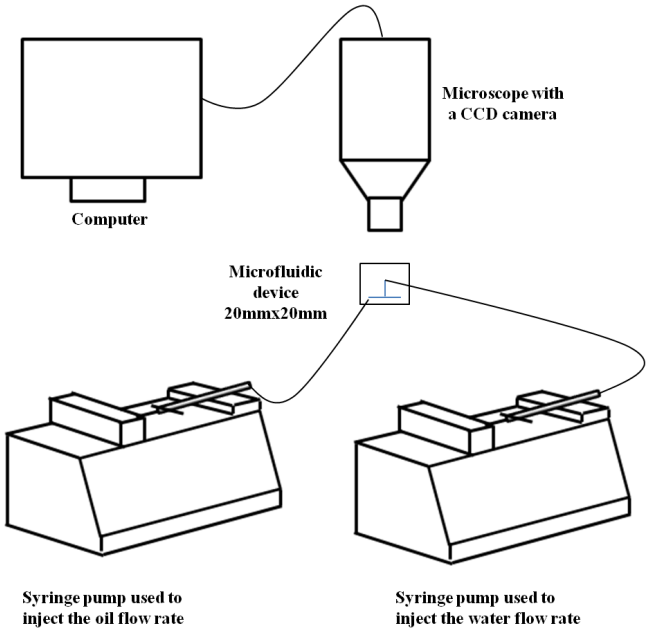

Fig. 2 Schematic of the experimental setup used to generate oil droplet in water in a T-junction microfluidic system.

3 Results and discussion

3.1 Mechanism of micro–droplet generation

The micro-droplet is generated at the intersection of the two channels, and forms a circular shape. Then the micro-droplet formed moves into the continuous phase micro–channel in the direction of the water stream (figure 3).

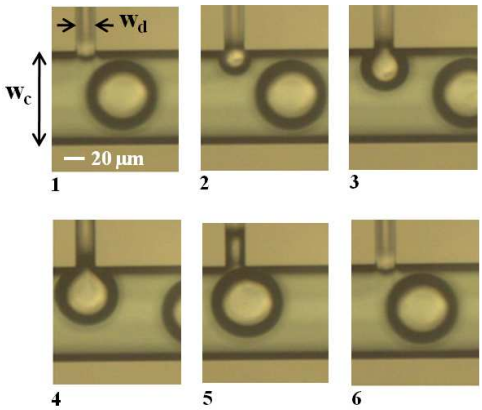

Fig. 3 Mechanism of micro–droplet formation in the balloon regime with $w_d = 20$ µm and $w_c = 100$ µm.

Actually, the micro–droplet generation process starts when the dispersed phase arrives at the T–junction, enters the continuous phase micro–channel and starts forming a circular shape. A similar step is present at the beginning of the dripping regime (figure 4). In the present regime, and contrary to the dripping regime, the micro–droplet continues its swelling without any deformation before it detaches. The origin of this behavior is thought to originate from the structural stability of the micro–droplet cylindrical shape compounded with the large interfacial tension present in our experiments. The arrival of the dispersed phase at low velocity can not induce deformation of the droplet, which maintains its circular shape throughout its growth. In the dripping regime, the velocity of the dispersed phase is higher and the larger momentum deforms the micro–droplet which becomes unable to resist the lateral drag force exerted by the continuous phase flow. Actually, in our experiments the drag force is pressure dominated as we use water for the continuous phase and its low viscosity makes the shear component much smaller.

We call the new regime the balloon regime because the swelling of the droplet resembles an inflating balloon.

When the micro–droplet inflates, the angle θ between the micro–droplet and the wall of the continuous phase micro–channel decreases. Because of the continuity of the interface between oil and water, this decrease results in the apparition of a water bulge on both side of the stream in the dispersed phase micro–channel (figure 5). This phenomenon is apparent in figure 3 as an increased length of the micro–droplet neck (dark region). When the induced side bulges finally meet in the dispersed phase micro–channel for $\theta = \theta_{min}$, the micro–droplet detaches. This angle θ_{min} depends mainly on the width of the dispersed phase micro–channel w_d. In some way the suggested mechanism resembles the capillary instability phenomenon. For a smaller w_d, the bulge meets earlier, the angle θ_{min} is larger resulting in smaller droplet (figure 5 a and b).

Then the continuous phase transports the micro–droplet in the continuous phase micro–channel and a new cycle of micro–droplet generation starts.

This new droplet formation principle implies that the micro–droplets size depends mainly on the geometry of the microfluidic devices, and does not present a significant dependence relative to the velocities of the continuous and dispersed phases.

3.2 Effect of dispersed and continuous phases velocities

The dispersed phase velocity $\overline{v}_d$ was varied from 0.01 to 30 mm/s, and the continuous phase velocity $\overline{v}_c$ was varied from 0.5 to 500 mm/s (corresponding to $5\text{x}10^{-6} < \text{Ca} < 5\text{x}10^{-3}$).

In the regimes of droplet generation mentioned in the introduction, the micro–droplet length L (squeez-

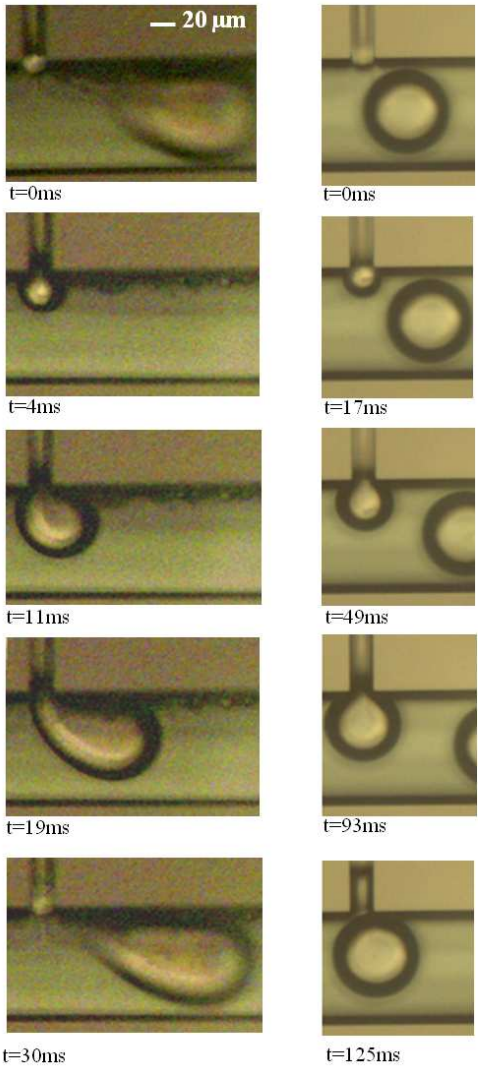

Fig. 4 Comparison between the process of the droplet formation in the dripping regime (left) for $\overline{v}_d$ = 15 mm/s, $\overline{v}_c$ = 72.5 mm/s (Tarchichi et al 2012), and the balloon regime (right) for $\overline{v}_d$ = 2.1 mm/s, $\overline{v}_c$ = 1.2 mm/s (w_d = 20 µm, w_c = 100 µm and h = 46 µm).

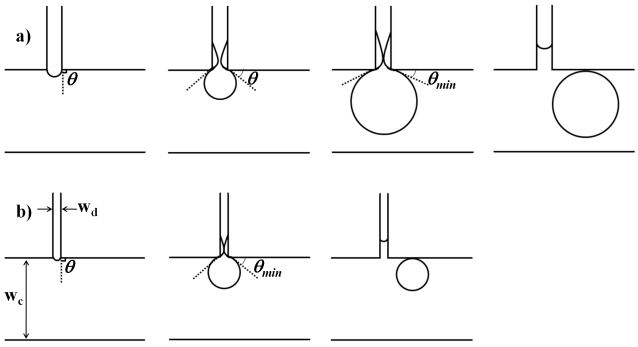

Fig. 5 Schematic of the micro–droplet detachment in the balloon regime with w_c = 100 µm and w_d = 20 µm (a), and 10 µm (b).

ing regime), and the micro–droplet diameter d (dripping regime), decreased when the velocity of the continuous phase $\overline{v}_c$ increased, but in the balloon regime, the diameter of the micro–droplet is constant and does not change when $\overline{v}_c$ changes. A comparison between the dripping regime and the balloon regime is presented in figure 6.

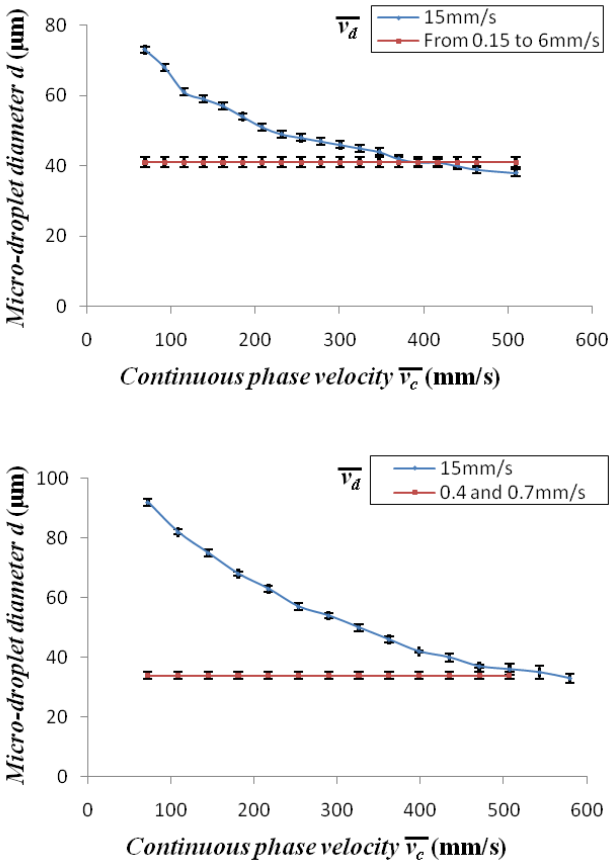

Fig. 6 Effect of the continuous phase velocity on the micro-droplet diameter in the dripping regime (Tarchichi et al 2012) and the new regime with w_c = 100 µm, w_d = 10 µm and h = 72 (a), 46 (b).

Actually, the continuous phase has two roles: the transport of the micro–droplet, and the control of its density. Figure 7 shows the distance l between two consecutive micro–droplets observed at very low values of the continuous phase velocity. At fixed $\overline{v}_d$, we found that l decreased when $\overline{v}_c$ decreased. Actually, the distance between two consecutive micro–droplets can be expressed as:

$$l = \frac{\overline{v}_c - df}{f} \tag{1}$$

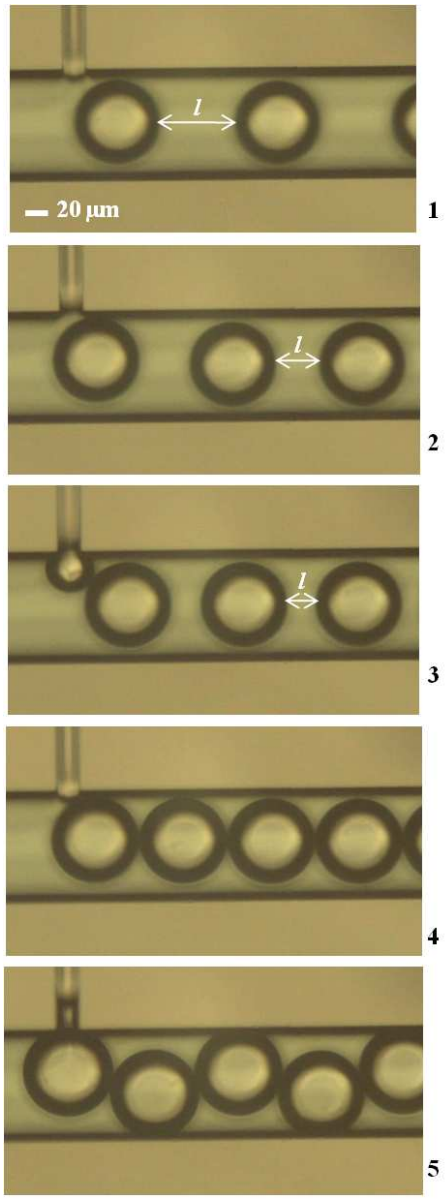

Fig. 7 Distance between two consecutive droplets with w_c = 100 µm, w_d = 20 µm, $\overline{v}_d$ = 2.1 mm/s and $\overline{v}_c$ = 1.2 mm/s (1), 1 mm/s (2), 0.85 mm/s (3), 0.65 mm/s (4) and 0.62 mm/s (5).

With f the frequency of the micro–droplet generation, which can be expressed by the following equation: $f = \frac{Q_d}{V_d}$, with Q_d the dispersed phase flow rate, and V_d the micro–droplet volume. We know that the dispersed phase flow rate is related to the dispersed phase velocity by: $Q_d = \overline{v}_d w_d h$. As the micro–droplet has a cylindrical shape, the micro–droplet volume can be expressed as: $V_d = \frac{\pi d^2 h}{4}$. So, we can write:

$$f = \frac{4 w_d}{\pi d^2} \overline{v}_d \qquad (2)$$

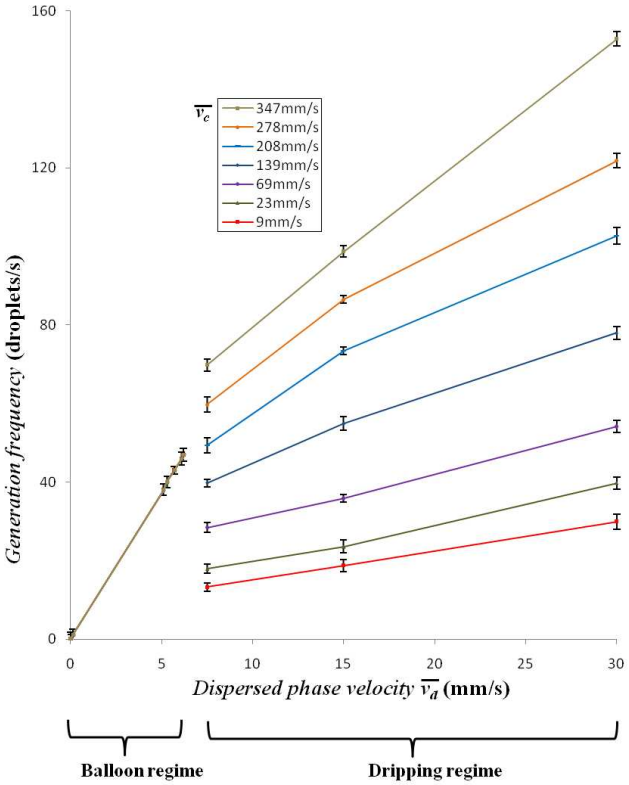

Fig. 8 Effect of the dispersed phase velocity on the frequency of the micro-droplet generation for different values of the continuous phase velocity with w_c = 100 µm, w_d = 10 µm and h = 72 µm.

Figure 8 allowed us to verify the linear dependence between the frequency and the dispersed phase velocity in the balloon regime (equation 2, d = constant), and confirming that the droplets have a quasi cylindrical shape. In addition the graph clearly shows the transition between the dripping regime and the balloon regime around $\overline{v}_d \approx 7$ mm/s.

3.3 Effect of geometry

We report in table 1 the micro-channels dimensions with which we have observed the balloon regime.

We observe that the micro-droplet diameter d depends on the depth and the width of the micro-channels. Based on the experimental data, we found that:

– At fixed h and w_c, the micro–droplet diameter d increased when w_d increased, but when w_d becomes larger, we do not observe the balloon regime (cf. (b, d, h) and (c, e, i)). Actually, when w_d increased, θ_{min} decreased, and the micro–droplet formed is larger. However, when the micro–droplet becomes too large it end up reaching the upper wall of the continuous phase micro–channel, deforming, and the dripping regime appears.

Experiments	$w_c(\mu m)$	$w_d(\mu m)$	$h(\mu m)$	Balloon regime
a	100	10	23	–
b	100	10	46	$d = 34\mu m$
c	100	10	72	$d = 41\mu m$
d	100	20	46	$d = 81\mu m$
e	100	20	72	$d = 88\mu m$
f	50	20	46	–
g	50	20	72	–
h	100	50	46	–
i	100	50	72	–

Table 1 Balloon regime for different geometry at low dispersed phase velocity (For large dispersed phase velocity, dripping regime appears in all cases).

– At fixed w_d and w_c, the micro–droplet diameter d decreased slowly when the micro–channel depth h decreased. Actually, as we clarified previously the apparition of the balloon regime is mainly related to the stability of the micro–droplet shape. When h decreases, the micro–droplet decreases its diameter d, in order to maintain the stability of its cylindrical shape while keeping the contact angle constraint at the top and bottom of the continuous phase micro–channel. As h becomes even lower, we could not observe the balloon regime at all. In this case, the micro–droplet can not retain a stable cylindrical shape, and the detachment is then controlled by the drag forces. The dripping regime is present (cf. (a, b, c)).

– At fixed micro–channel depth h and fixed width of the dispersed phase micro–channel w_d, we could observe the balloon regime when w_c was 100 µm, but could not when w_c was 50 µm (cf. (d, f) and (e, g)). In this last case, the diameter of the micro–droplet in the balloon regime would be larger than w_c, then it reaches the upper wall of the continuous phase micro–channel before it can detach. The balloon regime can not be observed.

4 Conclusion

In this study, we present a new regime of oil in water micro–droplet generation called balloon regime observed at lower values of the dispersed phase velocity. Several T–shape microfluidic junction with different cross–sections made on silicon–glass were fabricated in the clean room. In the balloon regime the droplets generated have a constant size, smaller than the width of the continuous phase channel, and independent of the continuous and the dispersed phase velocities. The continuous and the dispersed phases flow rates control the density and the generation frequency of the micro–droplet, respectively. We also presented a comparison between the dripping regime and the balloon regime to highlight the differences between their. In the dripping regime, the micro–droplet deforms before detachment and takes its circular shape in the continuous phase micro–channel at some distance from the T–junction. In the balloon regime, the micro–droplet takes its circular shape in the T–junction and undergoes no deformation. We finally proposed a mechanism explaining the generation of droplet in the balloon regime based on the stability of the micro–droplet shape.

References

Abate AR, Poitzsch A, Hwang Y, Lee J, Czerwinska J, Weitz DA (2009) Impact of inlet channel geometry on microfluidic drop formation. Physical Review E 80:026,310

Christopher GF, Noharuddin NN, Taylor JA, Anna SL (2008) Experimental observations of the squeezing–to-dripping transition in T–shaped microfluidic junctions. Physical Review E 78:036,317

Cristini V, Tan Y (2004) Theory and numerical simulation of droplet dynamics in complex flows–a review. Lab Chip 4:257–264

Cubaud T, Mason TG (2008) Capillary threads and viscous droplets in square microchannels. Physics of Fluids 20:053,302

Cubaud T, Tatineni M, Zhong X, Ho CM (2005) Bubble dispenser in microfluidic devices. Physical Review E 72:037,302

Dopierala K, Javadi A, Krägel J, Schano KH, Kalogiannid E, Leser M, Miller R (2011) Dynamic interfacial tensions of dietary oils. Colloids and Surfaces A 382:261–265

Fu T, Ma Y, Funfschilling D, Li HZ (2009) Bubble formation and breakup mechanism in a microfluidic flow-focusing device. Chemical Engineering Science 64:2392–2400

Gañán-Calvo AM, Gordillo JM (2001) Perfectly monodisperse microbubbling by capillary flow focusing. Phys Rev Lett 87:274,501

Garstecki P, Fuerstman MJ, Stonec HA, Whitesides GM (2006) Formation of droplets and bubbles in a microfluidic T–junction scaling and mechanism of break-up. Lab on chip 6:437–446

Glawdel T, Elbuken C, Ren CL (2012) Droplet formation in microfluidic T–junction generators operating in the transitional regime. Physical Review E 85:016,322

Gunther A, Jhunjhunwala M, Thalmann M, Schmidt MA, Jensen KF (2005) Micromixing of miscible liquids in segmented gas–liquid flow. Langmuir 21:1547–1555

Hashimoto M, Mayers B, Garstecki P, Whitesides GM (2006) Flowing lattices of bubbles as tunable, self-assembled diffraction gratings. Small 2:1292–1298

Menech MD, Garstecki P, Jousse F, Stone HA (2008) Transition from squeezing to dripping in a microfluidic T–shaped junction. journal of fluid mechanics 595:141–161

Nguyen N, Lassemono S, Chollet F, Yang Chun C (2007) Interfacial tension measurement with an optofluidic sensor. IEEE Sensors 7:692–697

Nisisako T, Torii T, Higuchi T (2002) Droplet formation in a microchannel network. Lab on a chip 2:24–26

Seong GH, Zhan W, Crooks RM (2002) Fabrication of microchambers defined by photopolymerized hydrogels and weirs within microfluidic systems: Application to DNA hybridization. Anal Chem 74:3372–3377

Sivasamy J, Wong TN, Nguyen NT, Kao LTH (2011) An investigation on the mechanism of droplet formation in a microfluidic T– junction. Microfluid Nanofluid 11:1–10

Tarchichi N, Chollet F, Manceau JF (2012) T–junction cross–section geometry influence on oil in water micro–droplets diameter. In preparation

Thorsen T, Roberts R, Arnold FH, Quake SR (2001) Dynamic pattern formation in a vesicle-generating microfluidic device. Phys Rev Lett 86:4163–4166

Umbanhowar PB, Prasad V, Weitz DA (2000) Monodisperse emulsion generation via drop break off in a coflowing stream. Langmuir 16:347–351